



ELSEVIER

Journal of Molecular Catalysis A: Chemical 121 (1997) 9–15

**JOURNAL OF
MOLECULAR
CATALYSIS
A: CHEMICAL**

Olefin hydrogenations with hydrido(phosphonite)cobalt(I) under photoirradiation and EHMO calculations for the phosphonite photodissociation process

Masayoshi Onishi ^{a,*}, Masahiro Yonekura ^a, Katsuma Hiraki ^a, Minoru Shugyo ^b,
Hiroyuki Kawano ^c, Hisayoshi Kobayashi ^d

^a Department of Applied Chemistry, Faculty of Engineering, Nagasaki University, Nagasaki 852, Japan

^b Department of Structural Engineering, Faculty of Engineering, Nagasaki University, Nagasaki 852, Japan

^c Graduate School of Marine Science and Engineering, Nagasaki University, Nagasaki 852, Japan

^d Department of Chemical Technology, College of Science and Industrial Technology, Kurashiki University of Science and The Arts, Kurashiki 712, Japan

Received 4 September 1996; accepted 15 November 1996

Abstract

Pyrex-filtered photoirradiation of hydrido(phosphonite)cobalt(I) $[\text{CoH}\{\text{PPh}(\text{OEt})_2\}_4]$ (CoHL_4) brought about catalytic olefin hydrogenations under a dihydrogen pressure of 6 kg/cm^2 , and a photogenerated coordinatively unsaturated transient species CoHL_3 was presumed to be the key-role-playing intermediate in the catalytic reaction cycles. EHMO calculations for the Cs-symmetric model complex $[\text{CoH}\{\text{PH}(\text{OH})_2\}_4]$ determined that photodissociation of a phosphonite ligand (L) proceeded in the equatorial direction, leading to the olefin incorporation on the equatorial site in the course of $[\text{CoH}(\text{olefin})\text{L}_3]$ intermediate formation.

Keywords: Olefin hydrogenation; Hydridocobalt(I); Phosphonite; Photocatalysis; EHMO calculation

1. Introduction

The photochemistry of transition-metal organometallic complexes has become an active area of research [1], and considerable efforts have been focused on the properties of the nascent short-lived photoproducts (see, for example, [2]), involving coordinatively unsaturated organometallic fragments with high catalytic activities [3,4]. The photoreactivity of

transition-metal hydride complexes seems to be one of the current topics in the organometallic photochemistry [1], and we have been interested in the photochemical properties of thermally inert and isolable hydride complexes with the rare-gas-type 18-electron configuration on the central metal ions [4]. We investigated hydrido(phosphonite)cobalt(I) $[\text{CoH}\{\text{PPh}(\text{OEt})_2\}_4]$ (CoHL_4) [5] (Fig. 1) and its Pyrex-filtered photoirradiation has shown efficient dissociation of a phosphonite ligand $\text{PPh}(\text{OEt})_2$ (L) from cobalt, producing a coordi-

* Corresponding author. Fax: +81-958-476749.

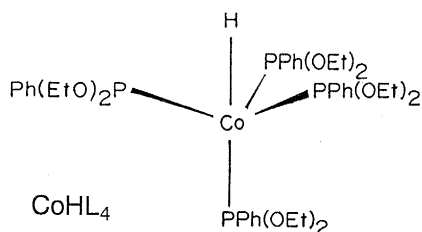


Fig. 1. The cobalt(I) complex of $[\text{CoH}(\text{PPh}(\text{OEt})_2)_4](\text{CoHL}_4)$.

natively unsaturated hydride transient species ‘ $\text{CoH}\{\text{PPh}(\text{OEt})_2\}_3$ ’ (CoHL_3) [4]. The catalytic activities of the CoHL_3 transient have been realized in several reactions, such as double-bond migration of some allylic compounds [4,6]. As another example of catalytic reactions mediated by the photogenerated CoHL_3 , the present paper deals with catalytic hydrogenations of olefins and some other related compounds with molecular hydrogen under a comparatively low pressure (6 kg/cm²). In addition, some quantum-mechanical molecular orbital calculations were carried out with an extended Hückel method modified with self-consistent charge refinements (scc EHMO) [7], to gain a clue to the phosphonite photodissociation mechanism from cobalt.

2. Experimental

2.1. Materials and general procedures

The cobalt complex CoHL_4 was prepared by the published procedures [5] with a slight modification. Determinations of catalytic reaction products and their quantitative evaluations were performed gas-chromatographically by comparison with authentic samples (Shimadzu GC-8AIT gas-chromatograph with a TCD detector, stainless steel columns packed with 10% PEG-20M on Chromosorb W NAW, 5% OV-17 on Uniport HP, and 10% Silicone SE-30 on Uniport B.). In addition, gas chromatograph–mass spectra (GC–MS) were observed also with a JEOL model JMS-DX-303 instrument.

2.2. Catalytic reactions

Test solutions of organic substrates and the catalyst were transferred through syringes into a 10 ml thick-walled A-2-type glass reactor (Taiatsu Scientific Glass Co.) under dinitrogen atmosphere. Then the reactor was evacuated with an aspirator for a short period and filled with dihydrogen under a high pressure, ca. 8 kg/cm². Release of dihydrogen to atmospheric pressure and its recharging up to the former high pressure were repeated three times. Hydrogenations of the test solutions were carried out at 50°C for 4 h in the reactor with magnetic stirring, under dihydrogen pressure of 6 kg/cm². During the reactions, the test solutions were photoirradiated by use of a 400 W high-pressure Hg lamp with a Pyrex filter.

2.3. Quantum mechanical calculations

Quantum mechanical molecular orbital calculations were performed with scc EHMO methods, by use of a NEC PC-9801RA computer. The program has been written by one of the authors (HK) [8]. For setting up the model $[\text{CoH}\{\text{PH}(\text{OH})_2\}_4]$, the geometry around the cobalt ion, besides Co–H and Co–P bond lengths, followed the single-crystal X-ray structural data of CoHL_4 [9]. Other geometrical parameters, such as P–H, P–O and O–H bond lengths, were from the literature [10]. The basis sets of the valence atomic orbitals were 3d, 4s, and 4p wavefunctions for cobalt, 3s and 3p for phosphorus, 2s and 2p for oxygen, and 1s for hydrogen, making up the 26-atom model complex with 90 electrons and 70 orbitals. These wavefunctions were expressed as Slater-type orbitals, and the resonance integrals were evaluated by using the Wolfsberg–Helmholtz expression ($K = 1.75$) [7,8]. The input parameters of valence state ionization potentials (VSIP) and Slater exponents have appeared in the literature [7,8,11].

3. Results and discussion

3.1. Catalytic hydrogenations of olefins and some related compounds

The hydridocobalt(I) complex CoHL_4 was combined with 200-fold moles of olefinic substrates in THF or in its mixture with ethanol (1/1). Test solutions of the complex and olefins were transferred through syringes into a thick-walled Pyrex pressure-bottle (10 ml), followed by charge with dihydrogen gas (6 kg/cm²). Hydrogenations of the olefins in the dark proceeded only a little, whereas Pyrex-filtered photoirradiation increased significantly the catalytic hydrogenation activities, as summarized in Table 1¹. The present olefin hydrogenations were best

described as photoassisted catalytic reactions [12], and the CoHL_3 species was presumed to work as the key-role-playing intermediate in these catalytic reaction-cycles also [4,6].

High yields of the hydrogenation reactions were brought about for monosubstituted terminal olefins, R-CH=CH_2 , such as allylbenzene and 5-hexene-2-one. Although olefin isomerization via double-bond migration was accompanied as a side pathway, the former substrate especially, disappeared completely through the reactions for 4 h. In case of a run performed with 1000-fold moles of allylbenzene for 4 h, where some quantity of allylbenzene was recovered unchanged, the turnover number (TN) per cobalt catalyst amounted to 196 for the hydrogenation. On the contrary, hydrogenations of β -methylstyrenes (internal olefins as its isomerization products) were not observed significantly. Hydrogenations of 5-hexene-2-one also proceeded well, yielding 2-hexanone in high yields, and a fair amount of this product was

¹ At 50°C, some quantities of isomerized olefins via double bond migration were fairly produced as by-products even in the dark, in contrast to the result performed at 30°C, where no olefin isomerization occurred without photoirradiation [4].

Table 1
Catalytic hydrogenations of olefins and some other related compounds^{a,b}

Run	Substrate	Products	T.N.			
			in THF		in THF/EtOH(1/1)	
			<i>hν</i>	dark	<i>hν</i>	dark
1	allylbenzene	<i>n</i> -propylbenzene	91.8	0.4	126.2	0.1
		(<i>E</i>)- β -methylstyrene	3.6	3.1	2.6	1.2
		(<i>Z</i>)- β -methylstyrene	104.1	17.5	70.9	7.1
2	5-hexene-2-one	2-hexanone	141.3	0.2	147.6	0.1
		2-hexanol	21.4	trace	25.5	trace
		isomerized hexene-2-ones	20.2	4.8	13.8	4.4
3	methyl vinyl ketone	methyl ethyl ketone	7.5	0	9.2	0
4	2-cyclohexene-1-one	cyclohexanone	3.6	0	4.9	0
5	methylenecyclohexane	methylcyclohexane			22.7	trace
6	α -methylstyrene	cumene			3.8	0
7	β -methylstyrenes	<i>n</i> -propylbenzene			3.9	0
8	cyclohexene	cyclohexane			3.7	0
9	diphenylacetylene	1,2-diphenylethane			trace	0
		(<i>Z</i>)-stilbene			17.6	0
		(<i>E</i>)-stilbene			6.3	0
10	1-phenyl-1-propyne	allylbenzene			trace	0
		β -methylstyrenes			trace	0
		<i>n</i> -propylbenzene			2.3	0

^a Conditions: 50°C, 6 kg/cm² (H_2), 4 h, $[\text{CoH}\{\text{PPh}(\text{OEt})_2\}_4]$, 10^{-3} M. Catalyst/Substrate: 1/200. Light source: 400 W high-pressure mercury lamp.

^b Under similar reaction-conditions, hydrogenations of diethyl fumarate, stilbenes and diethyl acetylenedicarboxylate were not proceeded significantly.

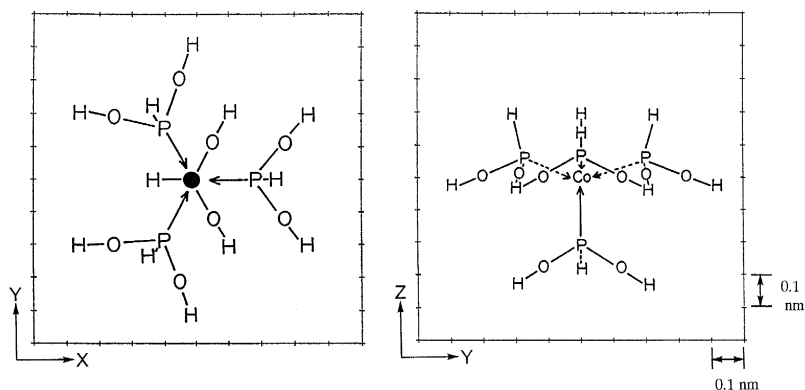


Fig. 2. XYZ three-dimensional configuration of $[\text{CoH}(\text{PH}(\text{OH})_2)_4]$. The origin of the coordinate axes is located on the central Co atom. Left: top view through $\text{H}-\text{Co}-\text{P}_{\text{ax}}$ bonds (the Z axis). Right: side view through the Y axis.

converted even further to an additionally carbonyl-hydrogenated compound, i.e. 2-hexanol.

As for methyl vinyl ketone and 2-cyclohexene-1-one, which have olefinic moieties conjugated with a π -delocalized carbonyl group, low electron-density on the $\text{C}=\text{C}$ bonds produced comparatively low hydrogenation yields. Among the other olefins examined, methylenecyclohexane, a representative of $\text{RR}'\text{C}=\text{CH}_2$, gave a moderate TN value of 22.7, whereas significant hydrogenations were not observed for diethyl fumarate and stilbenes.

Hydrogenation activities of the CoHL_4 complex under photoirradiation were investigated also for internal acetylenes, such as diphenylacetylene, 1-phenyl-1-propyne, and diethyl acetylenedicarboxylate, under reaction conditions similar to those performed for the olefins. Diphenylacetylene gave some quantities of (*E*)- and (*Z*)-stilbenes, classified as $\text{RCH}=\text{CHR}'$ olefins, and probably due to their steric hindrance, further hydrogenations to 1,2-diphenylethane were not advanced significantly. On the other hand, from the reaction with 1-phenyl-1-propyne, we found only a small amount of *n*-propylbenzene as a hydrogenated product, on the basis of gas chromatographic analyses. Hydrogenation of diethyl acetylenedicarboxylate was not proceeded.

Thus, the complex CoHL_4 under photoirradiation demonstrated catalytic hydrogenation ac-

tivities towards olefin and some other related compounds, with dihydrogen under a comparatively low pressure ($6 \text{ kg}/\text{cm}^2$). Among the substrates examined, terminal olefins showed high yields, but internal olefins afforded comparatively small amounts of hydrogenated products.

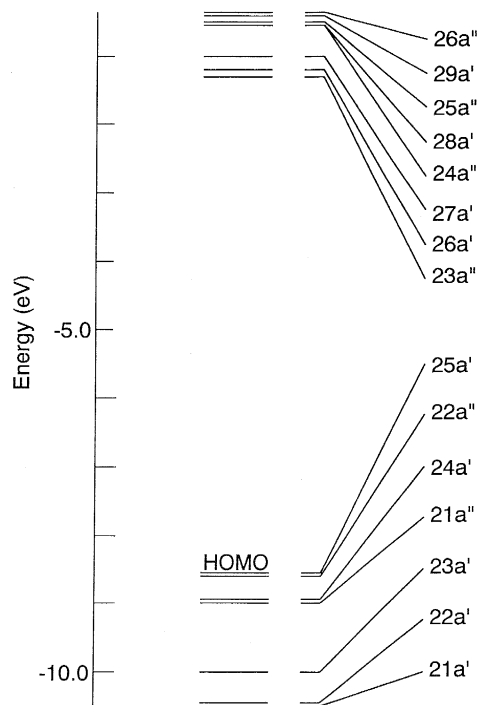


Fig. 3. Distribution of molecular orbital eigenvalues determined for $[\text{CoH}(\text{PH}(\text{OH})_2)_4]$ with sec EHMO methods.

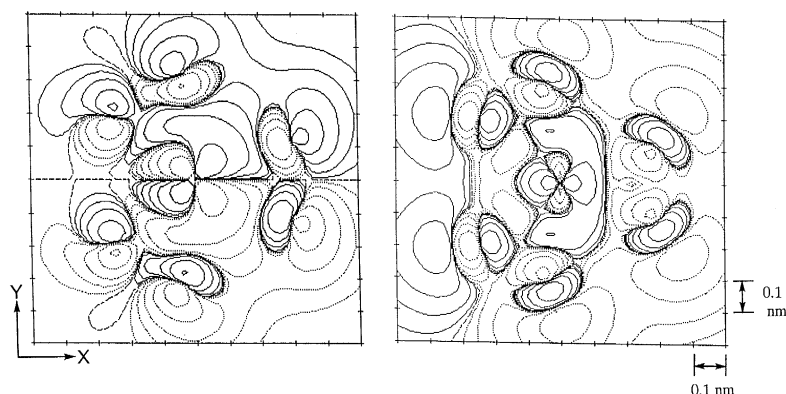


Fig. 4. Wavefunction contour plots for $[\text{CoH}\{\text{PH}(\text{OH})_2\}_4]$. Left: the horizontal section of $22a''$ on the Co-atom-involving XY plane. Right: the horizontal section of $26a'$ on the Co-atom-involving XY plane.

3.2. Molecular orbital calculations for the phosphonite photodissociation process

The mechanism of the phosphonite photodissociation process for CoHL_4 appeared to have been poorly understood so far. To find a clue to the mechanism, we undertook scc EHMO calculations [7,8] for the photodissociation process of $\text{PH}(\text{OH})_2$ from a C_s -symmetric model complex of $[\text{CoH}\{\text{PH}(\text{OH})_2\}_4]$ (Fig. 2).

The complex CoHL_4 has a pseudo trigonal bipyramidal structure [9] with an axial Co–H bond length of 0.138 nm and average $\angle\text{H}(\text{axial})\text{--Co--P}(\text{equatorial})$ angles of 76.9° . The Co–P bond lengths have been described as 0.2115 (as average) and 0.2128 nm in the equatorial and axial directions, respectively [9]. The model $[\text{CoH}\{\text{PH}(\text{OH})_2\}_4]$ was set up in accord with these structural characteristics of CoHL_4 , and its calculations led us to an energy diagram study for the photoexcited model complex, in the course of Co–P bond elongation toward axial and one equatorial² directions.

Fig. 3 shows eigenvalue, i.e. energy level distribution and primary symmetrical-characters of molecular orbitals of $[\text{CoH}\{\text{PH}(\text{OH})_2\}_4]$. The ground-state electron-configuration showed

$23a''$, $26a'$ and $27a'$ levels in the bottom energy-region for electron-unoccupied empty orbitals, and exhibited also $25a'$ and $22a''$ in the top energy-region for electron-occupied orbitals (Figs. 3 and 4). The electron-occupied $25a'$ orbital had primary cobalt p_x , $d_{x^2-y^2}$ and d_{xz} characters, and the $22a''$ orbital showed p_y , d_{xy} and d_{yz} ones. On the other hand, the electron-unoccupied vacant orbital $26a'$ bore phosphonite-ligand, in particular, oxygen-atom characters with small additional contributions by cobalt p_x , p_z and $d_{x^2-y^2}$ ones.

Upon Co–P bond elongation, the eigenvalue variations of $22a''$, $23a''$, $25a'$ and $27a'$ were found to be small. The variations due to 1.1 nm elongation were less than 0.1 and 0.4 eV for $22a''$ and $27a'$ and for $23a''$ and $25a'$, respectively. On the other hand, the unoccupied orbital of $26a'$ was considerably stabilized on the elongation. Co–P bond elongation by 1.1 nm showed about 3.6 eV stabilization increase for $26a'$. Symmetrically allowed one-electron transition through photoabsorption by the model complex is expected to occur between a' and a'' orbitals, and we determined the transition from $22a''$ to $26a'$, as the lowest-energy one-electron photoexcitation under discussion. Considerable stabilization of the $26a'$ orbital upon the Co–P elongation was the main driving force, leading to the phosphonite photodissociation.

The above-mentioned characters of these or-

² For clarity, the Co–P elongation in one equatorial direction was performed for the $\text{PH}(\text{OH})_2$ located on the XZ plane.

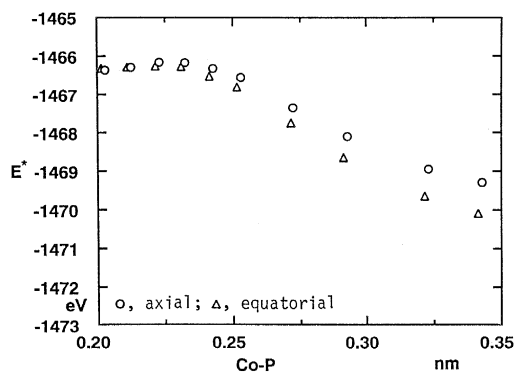


Fig. 5. E^* variations of $[\text{CoH}\{\text{PH}(\text{OH})_2\}_4]$ upon axial or one equatorial Co-P length changes. $E^* = E^0 - e^0(22a'') + e^*(26a')$.

bitals indicated also that the present photoexcitation from $22a''$ to $26a'$ was a metal-to-ligand charge transfer. Actually, the CoHL_4 in CH_2Cl_2 gave a charge-transfer-type absorption band (ϵ , 6400) around 340 nm, where photoirradiation of the complex has shown efficient formation of the coordinatively unsaturated CoHL_3 species [4,6].

Concerning the $26a'$ and $22a''$ orbitals, differences in the amounts of the eigenvalue variations were found to be very small, between two cases of axial and one equatorial phosphonite elongations from cobalt. On the contrary, destabilization of the total energy E^0 of the model with the ground-state electron-configuration was fairly different, whether Co-P elongation occurs in the axial or equatorial direction. Then, we evaluated total energy E^* for the one-electron photoexcited model complex from the following equation:

$$E^* = E^0 - e^0 + e^*,$$

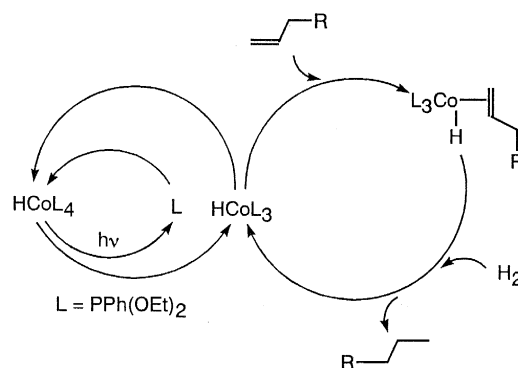
where e^0 is the eigenvalue of the orbital, from which one-electron photopromotion occurs, that was the orbital $22a''$, and e^* is the eigenvalue of the orbital occupied by the photopromoted electron, that was the orbital $26a'$ (Fig. 3).

Fig. 5 shows the E^* variations upon the changes in Co-P bond lengths in axial or one equatorial direction, and the equatorial elonga-

tion was found to bring about larger E^* stabilization, than the axial one. E^* - energy differences between the two directions were about 0.26 and 0.71 eV at the elongated Co-P bond lengths of 0.252 and 0.322 nm, respectively. These facts led us to conclude that phosphonite photodissociation from $[\text{CoH}\{\text{PPh}(\text{OEt})_2\}_4]$ occurred in the equatorial direction, rather than in the axial one, and the coordinatively unsaturated CoHL_3 transient species incorporated organic substrates through the photoproduced vacant equatorial coordination site.

4. Summary of the mechanistic profile

Pyrex-filtered photoirradiation of CoHL_4 dissociated one phosphonite ligand L to give the coordinatively unsaturated hydride CoHL_3 species. In olefin hydrogenations, the outstanding preference of the transient CoHL_3 species to olefins, which has been revealed as a characteristic feature by conspicuously large values of their second-order coordination-rate constants [4,13], indicated quick olefin incorporation on cobalt. The scc EHMO calculations for the model complex showed photodissociation of one equatorial phosphonite ligand, leading to the olefin incorporation on the equatorial site in the course of $[\text{CoH}(\text{olefin})\text{L}_3]$ intermediate formation. (Scheme 1).



Scheme 1.

Acknowledgements

The present work was partially supported by a Grand-in-Aid for Scientific Research (A) No. 07304076 and (C) No. 08650982 from the Ministry of Education, Science, and Culture in Japan.

References

- [1] G.L. Geoffroy and M.S. Wrighton, *Organometallic Photochemistry* (Academic Press, New York, 1979); J.J. Zuckerman, *Inorganic Reactions and Methods*, Vol. 15 (VCH Verlagsgesellschaft, Weinheim, 1986) ch. 13.
- [2] W.D. Jones and F.J. Feher, *J. Am. Chem. Soc.* 106 (1984) 1650; H.L. Conder, A.R. Courtney and D. DeMarco, *J. Am. Chem. Soc.* 101 (1979) 1606; A.S. Goldman and D.R. Tyler, *J. Am. Chem. Soc.* 108 (1986) 89; K.A. Mahmoud, A.J. Rest and H.G. Alt, *J. Chem. Soc. Dalton Trans.* (1984) 187; H. van der Heijden, A.G. Orpen and P. Pasman, *J. Chem. Soc. Chem. Commun.* (1985) 1576.
- [3] M.J. Mirbach, M.F. Mirbach, A. Saus, N. Topalsavoglou and T.N. Phu, *J. Am. Chem. Soc.* 103 (1981) 7590; M.A. Schroeder and M.S. Wrighton, *J. Am. Chem. Soc.* 98 (1976) 551.
- [4] M. Onishi, S. Oishi, M. Sakaguchi, I. Takaki and K. Hiraki, *Bull. Chem. Soc. Jpn.* 59 (1986) 3925, and references therein; M. Onishi, I. Takaki, K. Hiraki and S. Oishi, *J. Chem. Soc. Dalton Trans.* (1988) 2675.
- [5] D. Titus, A.A. Orio and H.B. Gray, *Inorg. Synth.* 13 (1977) 117.
- [6] M. Onishi, M. Matsuda, I. Takaki, K. Hiraki and S. Oishi, *Bull. Chem. Soc. Jpn.* 62 (1989) 2963.
- [7] The Chem. Soc. Japan, *Inorganic Quantum Chemistry*, in: *Kikan Kagaku Sosetsu*, No. 13 (Japan Scientific Societies Press, Tokyo 1991).
- [8] H. Kobayashi, *Shokubai (Catalysis)* 30 (1988) 267, and references therein.
- [9] D.D. Titus, A.A. Orio, R.E. Marsh and H.B. Gray, *J. Chem. Soc. Chem. Commun.* (1971) 322.
- [10] K. Lonsdale, *International Tables for X-ray Crystallography*, Vol. 3 (Kynoch Press, Birmingham, 1968), and references therein.
- [11] E. Clementi and D.L. Raimondi, *J. Chem. Phys.* 38 (1963) 2686; J.W. Richardson, W.C. Nieuwpoort, R.R. Powell and W.F. Edgell, *J. Chem. Phys.* 36 (1962) 1057; H. Basch, A. Viste and H.B. Gray, *Theoret. Chim. Acta* 3 (1965) 458; C.J. Ballhausen and H.B. Gray, *Molecular Orbital Theory* (Benjamin, Inc. New York, 1965).
- [12] L. Moggi, A. Juris, D. Sandrini and M.F. Manfrin, *Rev. Chem. Intermediates* 4 (1981) 171.
- [13] S. Oishi, N. Kihara and A. Hosaka, *Chem. Lett.* (1985) 621.